

Backscatter Sensor Network for Extended Ranges and Low Cost with Frequency Modulators: Application on Wireless Humidity Sensing

Eleftherios Kampianakis, John Kimionis, Konstantinos Tountas, Chris Konstantopoulos,
Eftichios Koutroulis and Aggelos Bletsas
ECE Dept., Technical University of Crete, Chania, Greece 73100
{ekabianakis, ikimionis, ktountas, ckonstantopoulos}@isc.tuc.gr,
efkout@electronics.tuc.gr, aggelos@telecom.tuc.gr

Abstract—Dense monitoring of environmental parameters (e.g. air/soil humidity, ambient temperature) is critical in precision agriculture, urban area monitoring and environmental modeling applications. In this paper, the design of a novel wireless sensor network (WSN) is proposed, consisting of low-power and low-cost sensor nodes, deployed in a bistatic architecture (i.e. carrier emitter in a different location than the receiver) and achieving long-range backscatter communication. The tags modulate sensor information using analog frequency modulation (FM) and frequency division multiple access (FDMA) at the *subcarrier* frequency, even though a single carrier is assumed. In sharp contrast to prior art, the developed backscatter sensor network performs environmental monitoring over a relatively wide area. A proof-of-concept prototype WSN application has been developed for capacitive relative humidity (RH) sensing, with 1.5 mW per tag, 0.9 RMSE and range on the order of 50 m.

I. INTRODUCTION

Wireless sensor networks (WSNs) have become a field of tremendous research interest due to a rich and diverse variety of applications, including large-scale environmental sensing [1], [2]. A common WSN platform typically consists of a micro-controller unit (MCU) and an active radio for sensor data transmission. Despite the fact that literature develops algorithms and protocols for ultra large-scale networks, on the order of hundred of nodes, large-scale outdoor demonstration deployments are rare. Work in [3] demonstrated one of the very few examples of a large-scale, outdoor deployment. However each node *cost* was on the order of 50 €, amplifying the overall network cost and thus, restricting scaling opportunities. Additionally, work in [4] studied the complexity of cross-layer application development in typical WSN platforms and emphasized the difficulty to implement software for robust sensor networks.

On the other hand, recent work relevant to backscatter radio has shown significant progress towards low-cost and low-power sensing (e.g. work in [5]–[8]). Backscatter communication can be implemented with a single antenna, a switching transistor and logic that controls that switch, such that the sensor's antenna is alternatively terminated at different loads. However, inductive coupling and/or monostatic battery-less setups result in short communication range, limiting the use

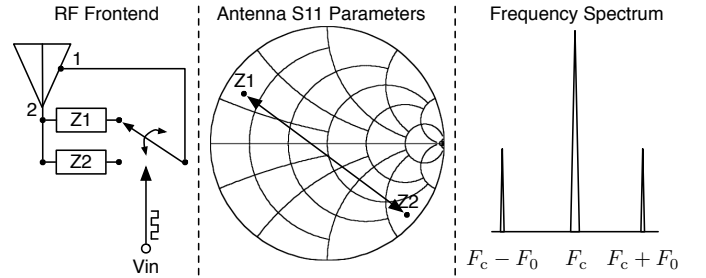


Fig. 1. Backscatter radio principle: a single, low-cost RF switch is utilized that alternates the antenna termination load between two values (left). Different antenna termination loads offer different reflection coefficients (i.e. S11 parameter, middle) that modulate the induced carrier signal (at frequency F_c) with different amplitude and phase. Switching frequency between the two load states varies with the measured quantity and is called *subcarrier* frequency, F_0 .

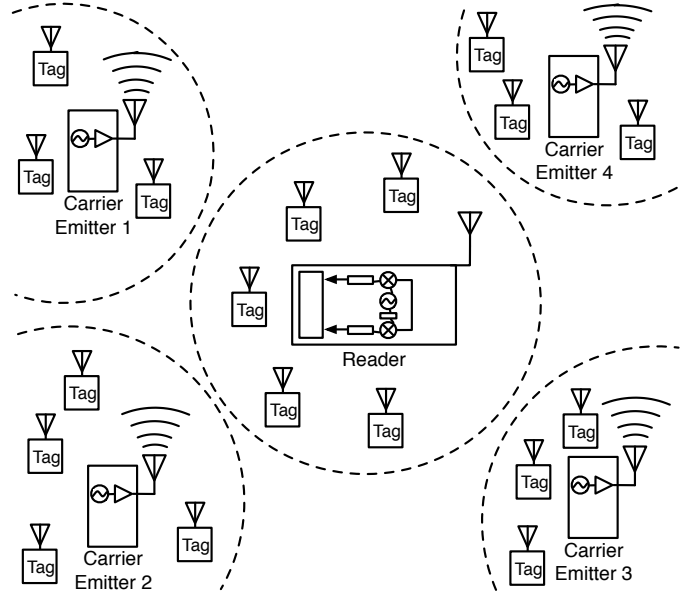


Fig. 2. Bistatic backscatter sensor network architecture. Low-cost carrier emitters produce the carrier, tags modulate the scattered signals received by a single reader (receiver).

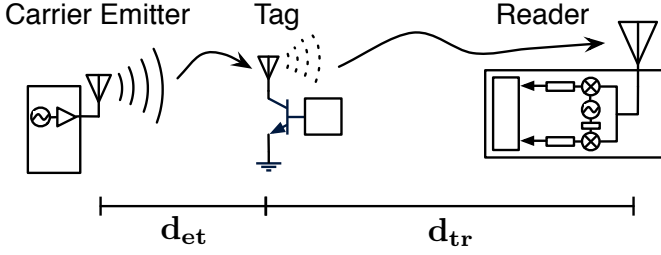


Fig. 3. Ranges measured in bistatic topology (i.e. carrier emitter dislocated from reader). d_{et} and d_{tr} denote the emitter-to-tag and tag-to-reader distance, respectively. $d_{et} = 10$ m and $d_{tr} = 50$ m with a 0.9 %RH RMSE for 30 %RH were achieved.

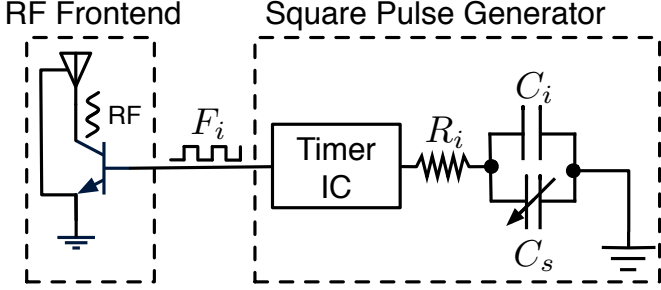


Fig. 4. Design of a backscatter radio-enabled tag/sensor. On the right-hand side the square pulse generator circuit is shown. On the left-hand side the RF front-end is depicted, implemented with a single RF switching transistor.

of backscatter radio for broad-area environmental sensing.

In contrast to prior art, this work develops a low-complexity, low-power and low-cost wireless humidity sensing tag that employs bistatic semi-passive scatter radio principles [9]. The network tag is evaluated in terms of accuracy and communication range and a proof-of-concept relative humidity (%RH) sensor is demonstrated.

Section II describes the design principles, Section III offers achieved range, accuracy, power and cost, and finally, Section IV concludes this work.

II. DESIGN

Backscatter radio is implemented with a single switch that alternatively terminates the tag/sensor antenna between typically two loads (Fig. 1). The antenna S11 parameter (i.e. reflection coefficient), associated with each antenna terminating load, is modified when the antenna load is changed, thus modulating the amplitude and phase of the carrier signal induced at the tag/sensor antenna and reflected back to the receiver. If the alternating (i.e. switching) frequency between the two loads is controlled, then the scattered signal will be frequency modulated (FM). Assuming carrier frequency F_c and transistor switching frequency F_0 , the frequency of the two *subcarrier* signals is:

$$\begin{aligned} F_{\text{sub1}} &= F_c + F_0 \\ F_{\text{sub2}} &= F_c - F_0. \end{aligned}$$

If the switching frequency of the transistor is a monotonic function of the parameter to be sensed, then wireless

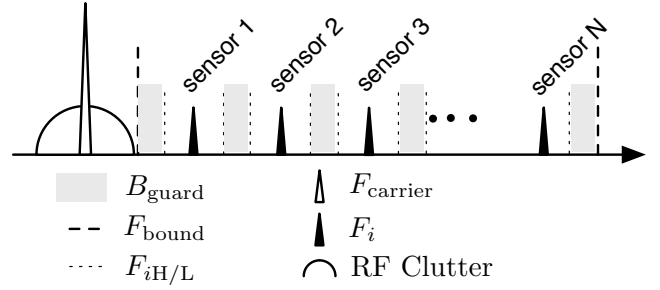


Fig. 5. Sensor network frequency division multiple access (FDMA). Guard bands between sensor bands are included for better collision avoidance of neighboring (in subcarrier frequency) tag/sensors.

sensing through analog backscatter becomes possible. This work proposes a bistatic architecture, i.e. the carrier emitter is dislocated from the receiver, as depicted in Fig. 2. Low-cost portable carrier emitters are dispensed in a broad geographical area, while a single, software-defined receiver processes the scattered signals from a multitude of backscatter-enabled sensor/tags around the emitters and the receiver. Such design promotes scalability, since the proposed sensor/tags have significantly less cost and power consumption than traditional WSN terminals, due to the lack of an active, conventional radio, i.e. no need for an RF front-end with power amplifiers, mixers, filters etc. Since a bistatic (instead of a monostatic) architecture is utilized (Fig. 3), communication ranges are extended to several tens of meters [9], [10].

The proposed tag design is based on low-cost and low-power relative humidity (%RH) to frequency modulator. A capacitive %RH sensor is connected through an RC network to a timer integrated circuit. The timer acts as a generator of variable frequency pulses based on %RH. Thus, frequency modulation (FM) is achieved. The modulated humidity signal is routed to the RF switch transistor controlling the antenna load termination (Fig. 4). The output frequency of the pulse generator as a function of the passive components (R_i , C_i) and the capacitance value of the sensor (C_s) is given by:

$$F_i = \frac{1}{\ln 2 R_i (C_i + C_s)}. \quad (1)$$

Each i -th tag can occupy bandwidth on the order of few kHz and is allocated a unique subcarrier frequency center, by selecting a specific pair of R_i , C_i . Thus, backscatter-enabled sensors directly implement frequency division multiple access (FDMA) and thus, offer receiver-less (at the tag), simultaneous, collision-free transmission from multiple tags [6], [11]. Equations (2) and (3) describe capacitor and resistor values:

$$C_i = \frac{B_i C_L + F_{iL} (C_H - C_L)}{B_i}, \quad (2)$$

$$R_i = \frac{B_i}{\ln 2 F_{iL} (C_H - C_L) (F_{iL} + B_i)}, \quad (3)$$

where B_i is the size of the corresponding frequency band (in Hz), C_H , C_L the value of the sensor for RH=100 % and 0 % respectively and F_{iL} is the low subcarrier frequency bound of

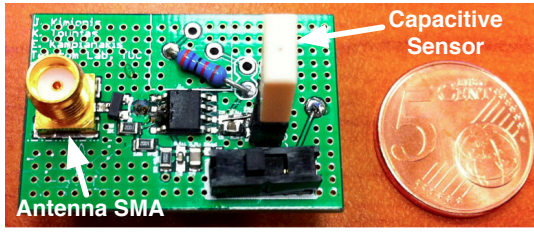


Fig. 6. Backscatter radio-enabled tag prototype with humidity capacitive sensor.

the i -th tag, produced for $C_s = C_H$. Fig. 5 depicts the FDMA scheme that tags implement. Frequency guard-bands between sensor bands offer collision avoidance. Each tag's subcarrier (i.e. switching) frequency estimation at the receiver is based on *periodogram* spectral estimation [12].

Eq. (1) describes the output frequency of the oscillator circuit, as a function of C_s ; the latter varies with relative humidity. However, due to manufacturing non-idealities, calibration is required for measurement accuracy. The output frequency of the tag is monitored for a broad range of %RH values. Humidity is measured with a reference industrial humidity sensor. The frequency output of the tag is directly measured at the receiver, thus communication errors are also considered in the calibration process. The output of the reference sensor is then compared to the output frequency of the wireless tag measured at the receiver, using polynomial curve fitting. Finally, the frequency values monitored at the receiver are converted to relative humidity through the produced characteristic function, and compared against the reference %RH. Root mean square error (RMSE) results are presented in the following section.

III. EXPERIMENTAL RESULTS

Tags were prototyped based on the above design and fabricated in-house (Fig. 6). Unique pairs of R_i and C_i were calculated for each sensor/tag i , according to (2) and (3), so that tags operate simultaneously in distinct frequency bands, without collision. Minimum effort was needed for setting up such network, since tags were set up for FDMA during fabrication; such a task was very simple.

Power consumption was measured on the order of 1.5 mW per tag, thus operation is sustainable for 170 days of *continuous* operation, with a 2500 mAh battery. It is important to note that traditional WSN nodes utilize duty cycling and occasionally transmit data (e.g. once per hour). That is critical for traditional WSNs, since duty cycling allows operation for long periods of time with power consumption on the order of tenths of mW (packet transmission). On the other hand, simultaneous, continuous (i.e. 100 % duty cycle) data backscattering from all tags of the proposed network is feasible over long periods of time, due to the lower power consumption.

Balancing between cost, power consumption and efficiency is not a trivial task for such applications and a significant amount of time was dedicated in finding the appropriate components for the design. A relatively low cost in bill of materials (BOM) of 5 € per tag is the result of the conducted

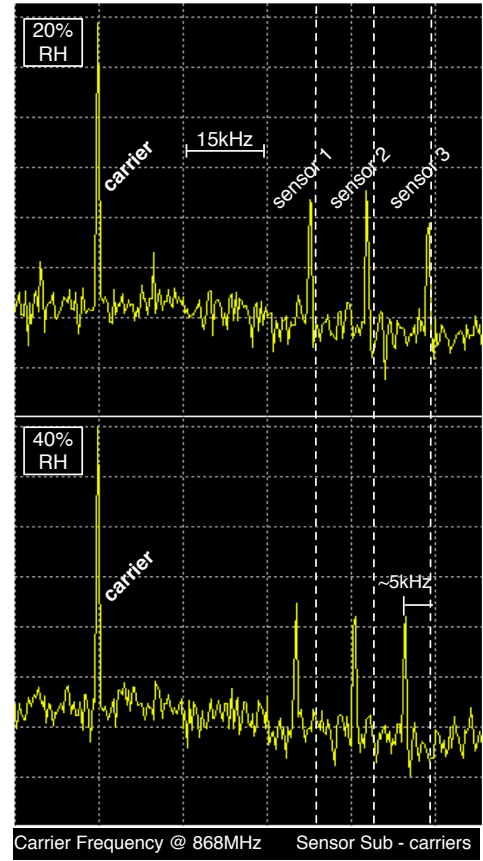


Fig. 7. Sensor network spectrum for sensors 1, 2 and 3 for 20 % and 40 % RH. The subcarrier frequency change is 5 kHz.

market research. The BOM includes the sensing element and excludes the SMA antenna connector, since in future designs the antenna will be integrated with the tag circuitry.

A proof-of-concept network of three tags was set up in order to evaluate the FDMA operation presented in Section II. The spectra of the backscattered signals from three sensors operating simultaneously are depicted in Fig. 7. Frequency shifting of the produced subcarriers is prominent when relative humidity changes from 20 % to 40 % while signal collision is obviously avoided.

A single tag was calibrated using the aforementioned procedure (i.e polynomial fitting) for a range of 20 %RH to 90 %RH humidity. Using the characteristic function depicted in Fig. 8, the % RH results was compared to a reference humidity sensor. An RMSE of 0.86 %RH and a mean error of 0.64 %RH were measured.

Communication range measurements for a single tag were conducted outdoors, using the setup of Fig. 9. The network terminals were set according to a bistatic topology and the operating range was measured in a real world environment with the system evaluated end-to-end (i.e. transmitter to reader). The industrial humidity sensor was utilized in order to compare the %RH results of the tag. Long communication ranges were experimentally verified: a 10 m emitter-to-tag and 50 m tag-to-reader range were achieved. At those distances,

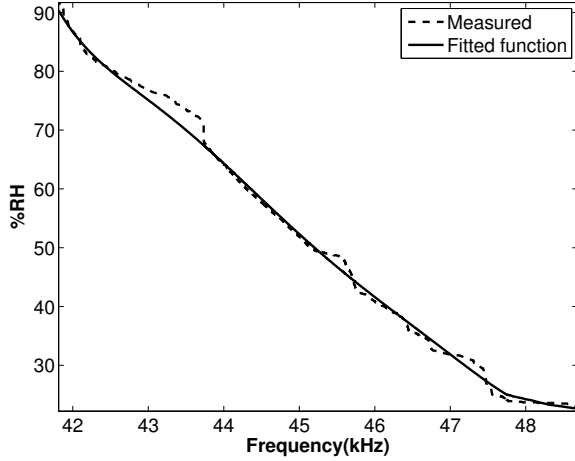


Fig. 8. Frequency-%RH characteristic for 20-90 %RH. RMSE = 0.86 %RH and mean error = 0.63 %RH with respect to a reference industrial RH sensor.

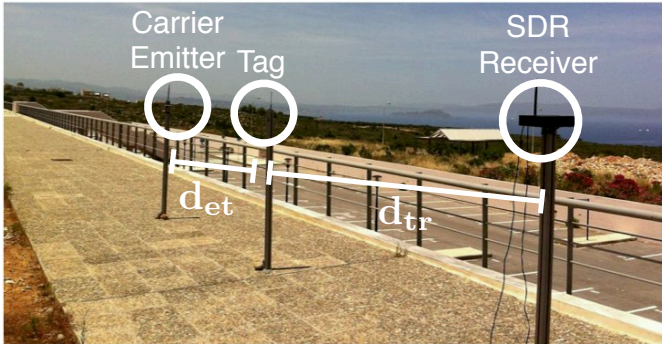


Fig. 9. Outdoor setup for communication range measurements of the bistatic analog backscatter architecture.

the RMSE was 0.9 %RH (30 %RH).

IV. CONCLUSION

A network architecture of backscatter radio-enabled sensors that consume 1.5 mW power was presented, with communication range exceeding 50 m. A proof-of-concept network was deployed, demonstrating simultaneous, collision-free operation, using (subcarrier) frequency division multiple access. Finally, the in-house prototype tag offered humidity measurements with RMSE of 0.86 %RH. Future work will target at a large-scale network outdoor demonstration.

ACKNOWLEDGMENT

This work was supported by the ERC-04-BLASE project, executed in the context of the Education & Lifelong Learning Program of General Secretariat for Research & Technology (GSRT) and funded through European Union-European Social Fund and national funds.

REFERENCES

- [1] G. Tolle, J. Polastre, R. Szewczyk, D. Culler, N. Turner, K. Tu, S. Burgess, T. Dawson, P. Buonadonna, D. Gay, and W. Hong, "A macroscope in the redwoods," in *Proceedings of the 3rd International Conference on Embedded Networked Sensor Systems*, ser. SenSys '05, 2005.
- [2] W.-Z. Song, R. Huang, M. Xu, B. Shirazi, and R. LaHusen, "Design and deployment of sensor network for real-time high-fidelity volcano monitoring," *IEEE Transactions on Parallel and Distributed Systems*, vol. 21, no. 11, pp. 1658–1674, 2010.
- [3] Y. Liu, Y. He, M. Li, J. Wang, K. Liu, L. Mo, W. Dong, Z. Yang, M. Xi, J. Zhao, and X.-Y. Li, "Does wireless sensor network scale? a measurement study on greenorbs," in *INFOCOM, 2011 Proceedings IEEE*, Shanghai, China, 2011.
- [4] L. Mottola and G. P. Picco, "Programming wireless sensor networks: Fundamental concepts and state of the art," *ACM Computer. Surv.*, vol. 43, no. 3, pp. 19:1–19:51, Apr. 2011.
- [5] A. Sample, D. Yeager, P. Powlledge, and J. Smith, "Design of a passively-powered, programmable sensing platform for uhf rfid systems," in *IEEE International Conference on RFID 2007*, Mar. 2007, pp. 149–156.
- [6] G. Vannucci, A. Bletsas, and D. Leigh, "A software-defined radio system for backscatter sensor networks," *IEEE Trans. Wireless Commun.*, vol. 7, no. 6, pp. 2170–2179, Jun. 2008.
- [7] V. Lakafosis, A. Rida, R. Vyas, L. Yang, S. Nikolaou, and M. Tentzeris, "Progress towards the first wireless sensor networks consisting of inkjet-printed, paper-based rfid-enabled sensor tags," *Proceedings of the IEEE*, vol. 98, no. 9, pp. 1601–1609, Sep. 2010.
- [8] D. Cirmirakis, A. Demosthenous, N. Saeidi, and N. Donaldson, "Humidity-to-frequency sensor in CMOS technology with wireless readout," *IEEE Sensors Journal*, vol. 13, no. 3, pp. 900–908, 2013.
- [9] J. Kimionis, A. Bletsas, and J. N. Sahalos, "Bistatic backscatter radio for tag read-range extension," in *IEEE International Conference on RFID-Technologies and Applications (RFID-TA)*, Nice, France, Nov. 2012.
- [10] J. Kimionis, A. Bletsas, and J. N. Sahalos, "Bistatic backscatter radio for power-limited sensor networks," in *Proc. IEEE Globecom*, Atlanta, USA, Dec. 2013.
- [11] A. Bletsas, S. Siachalou, and J. Sahalos, "Anti-collision tags for backscatter sensor networks," in *38th European Microwave Conference (EuMC)*, Amsterdam, Netherlands, Oct. 2008, pp. 179–182.
- [12] P. Stoica and R. Moses, *Spectral Analysis of Signals*. Prentice-Hall International, 1st ed., 2005.